THE JOURNAL OF PHYSICAL CHEMISTRY C

Article

pubs.acs.org/JPCC

Hydrogen and Hydrogen Peroxide Formation in Trifluorotoluene–Water Biphasic Systems

Wojciech Adamiak,*[,†] Justyna Jedraszko,[†] Olga Krysiak,[†] Wojciech Nogala,[†] Jonnathan C. Hidalgo-Acosta,[‡] Hubert H. Girault,[‡] and Marcin Opallo*[,†]

[†]Institute of Physical Chemistry, Polish Academy of Sciences, Kasprzaka 44/52, 01-224 Warsaw, Poland

[‡]Laboratoire d'Electrochimie Physique et Analytique, Ecole Polytechnique Federale de Lausanne, CH-1015 Lausanne, Switzerland

Supporting Information

ABSTRACT: Hydrogen or hydrogen peroxide can be generated in liquid–liquid biphasic systems, where the organic phase contains sufficiently strong electron donor (whose redox potential is lower than the potential of reversible hydrogen electrode). H_2O_2 generation with acidified aqueous phase occurs prior to H_2 evolution when oxygen is present. No other organic solvent than highly toxic 1,2-dichloroethane (DCE) has been reported in biphasic system for H_2 or H_2O_2 generation. In this work, we have used trifluorotoluene (TFT) instead of carcinogenic DCE, and studied these reactions in TFT–water biphasic system. To evaluate H_2 flux, scanning electrochemical microscopy potentiometric approach curves to the TFT–water interface were recorded. H_2O_2 was detected voltametrically at a microelectrode located in the vicinity of the interface. H_2 and H_2O_2 are formed and both reactions occur also in the absence of a hydrophobic salt in the organic phase. Their thermodynamics was discussed on the basis of Gibbs energies determined electrochemically with droplet-modified electrodes. The results show that DCE can be replaced by a noncarcinogenic solvent and the biphasic system for H_2 and H_2O_2 generation can be simplified by elimination of the uncommon hydrophobic salt from the organic phase.

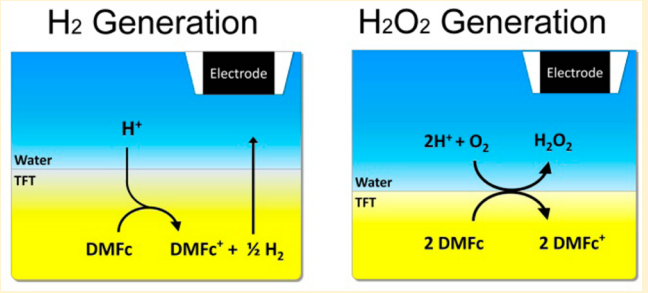

INTRODUCTION

Hydrogen and hydrogen peroxide are important chemicals used worldwide. Hydrogen is mainly used as a fuel,[1] whereas hydrogen peroxide is commonly used in chemical industry.[2] The most common industrial method of hydrogen production is the steam reforming process that requires a metal catalyst, like nickel, and a temperature as high as 700–1100 °C.[3] Hydrogen peroxide is produced industrially mainly with the anthraquinone process, which involves catalytic reduction of oxygen, followed by extraction of H_2O_2 from the organic reaction mixture to the aqueous phase.[4] The anthraquinone process requires hydrogen, which is highly desired in other processes or for power generation.

It has been shown that both H_2[5−10] and H_2O_2[11−13] can be produced in liquid–liquid biphasic systems comprising a polarized interface between two immiscible electrolyte solutions (ITIES). The reaction involves reduction of protons or oxygen dissolved in the aqueous phase by a metallocene dissolved in the adjacent organic phase. Hydrogen evolution reaction (HER) in the biphasic system can be more advantageous than steam reforming method, because of the absence of the metal catalyst and lower temperature required to drive the process. In contrast to the anthraquinone process, H_2O_2 formation in biphasic systems does not need hydrogen and H_2O_2 extraction step is eliminated, because the produced H_2O_2 is already dissolved in water after the reaction.

So far, research on HER and H_2O_2 formation at liquid–liquid interfaces has been restricted to the 1,2-dichloroethane-water (DCE-W) biphasic system.[5−13] DCE|W interface was polarized either chemically[5−10,13] or potentiostatically[5,6,8−10,12] to facilitate H^+ transfer from W to DCE. In case of chemical polarization, the Galvani potential difference between the organic and the aqueous phase, $\Delta_{aq}^{org}\phi$:[14]

$$\Delta_{aq}^{org}\varphi = \Delta_{aq}^{org}\varphi_i^{O} + \frac{RT}{z_iF}\ln\frac{a_i(aq)}{a_i(org)} \quad (1)$$

(where $\Delta_{aq}^{org}\phi_i^{o}$ is the standard potential of transfer of ion i from the aqueous to the organic phase, R is the gas constant, F is the Faraday constant, z_i is the charge number of ion i, a_i (aq) and a_i (org) are the activities of ion i in the aqueous and the organic phase, respectively), was lower than the proton transfer potential. Under these conditions, HER or H_2O_2 formation proceeds as a proton coupled electron transfer (PCET) reaction in the bulk organic phase with decamethylferrocene as a reducing agent. The reaction mechanism was also discussed with a help of density functional theory.[15] HER has been found

Received: July 22, 2014
Revised: September 16, 2014
Published: September 18, 2014

   dx.doi.org/10.1021/jp507310d | J. Phys. Chem. C 2014, 118, 23154–23161

Table 1. Values of Square Wave Voltammetry Peak Potentials (E_p) Obtained with Droplet-Modified Electrodes and the Estimated Values of Transferring Ion Potentials $\Delta_W^{TFT}\phi_i^{\ominus}$ and Gibbs Free Energies $\Delta_W^{TFT}G_i^{\ominus}$ (See Text for Details)

transferring ion	organic electrolyte[a]	aqueous electrolyte[b]	E_p/V[c]	$\Delta_W^{TFT}\phi_i^{\ominus}$/V	$\Delta_W^{TFT}G_i^{\ominus}$/kJ mol^{-1} [d]
$TPAs^+$	TPAsTPBCl	TPAsCl	0.204	0.224	−21.6
TPB^-	THepATPB	NaTPB	−0.361	−0.224	−21.6
TBA^+	TBATPB	TBACl	0.174	0.181	−17.4
$THxA^+$	$THxAClO_4$	THxACl	0.345	0.406	−39.2
TB^-	BATB	LiTB	−0.754	−0.616	−59.4
ClO_4^-	$TOAClO_4$	$NaClO_4$	0.097	0.235	22.7
SCN^-	TPenASCN	NaSCN	0.149	0.287	27.7
Br^-	TOABr	KBr	0.325	0.463	44.7
Cl^-	TOACl	KCl	0.409	0.547	52.8

[a]Concentration of organic electrolyte was 1 mM, except for 0.6 mM TBATPB. [b]Concentration of aqueous electrolyte was 10 mM, except for 1 mM THxACl. [c]Measured vs Ag|AgCl|3 M KCl in the aqueous phase. [d]Calculated from eq 4

to be facilitated by nanomaterials deposited at the DCE|W interface.[7,8,16]

Although DCE has been classified by International Agency of Research on Cancer as a carcinogen,[17] the use of less toxic solvents has not been reported. Trifluorotoluene (TFT), whose carcinogenic properties has not been reported, was proposed as an alternative solvent for ion transfer studies.[18] The Gibbs energies of ion transfer across water-organic interface are expected to be similar for both solvents, because of their similar polarity (the relative dielectric permittivities of TFT and DCE are 9.2[19] and 10.36,[20] respectively). Therefore, the PCET reactions like HER or H_2O_2 formation are also likely to occur at TFT|W interface. Additionally, TFT is less volatile than DCE (vapor pressure of TFT is 53 hPa at 25 °C[21] and for DCE is 85 hPa at 20 °C[22]), which is advantageous for the stability of the liquid|liquid interface.

The aim of this work was to investigate whether HER and H_2O_2 formation occurs in the TFT−W biphasic system. An attempt to simplify the biphasic system by elimination of the electrolyte from the organic phase has also been made. H_2O_2 formation with the aqueous phase containing no additional solutes except a proton donor, and the organic phase containing only an electron donor was confirmed. The effect of aqueous electrolyte and chemical polarization of the interface on HER and H_2O_2 formation will be discussed on the basis of thermodynamic parameters obtained with droplet-modified electrodes[23] and product fluxes obtained by scanning electrochemical microscopy (SECM).[24]

EXPERIMENTAL SECTION

Chemicals. Decamethylferrocene (DMFc, 97%) was purchased from ABCR. α,α,α-Trifluorotoluene (TFT, ≥99%) lithium tetrakis(pentafluorophenyl)borate ethyl etherate (LiTB), tetraoctylammonium bromide (TOABr, 98%), tetraoctylammonium chloride (TOACl, 97%), potassium tetrakis(4-chlorophenyl)borate (KTPBCl, 98%), 70% $HClO_4$, and bis(triphenylphosphoranylidene)ammonium chloride (BACl, 97%) were purchased from Sigma-Aldrich. Tetraheptylammonium tetraphenylborate (THepATPB, Selectophore), sodium tetraphenylborate (NaTPB, Selectophore), tetrabutylammonium tetraphenylborate (TBATPB, 99%), tetrabutylammonium chloride (TBACl, 97%), tetrahexylammonium chloride (THxACl, 96%), tetraoctylammonium perchlorate ($TOA^+ClO_4^-$, purum), tetrapentylammonium rhodanide (TPenASCN, 99%), NaCl (>99.99%), $NaClO_4$ (>99%), and NaSCN (purum) were purchased in Fluka. Tetraphenylarsonium chloride (TPAsCl, 99%) was purchased from Strem Chemicals. KBr (pure p.a.) was purchased in POCh. All chemicals were used as received. Tetraphenylarsonium tetrakis(4-chlorophenyl)chloride (TPAsTPBCl) was synthesized from TPAsCl and KTPBCl by metathesis and purified by two recrystallizations from acetone. Tetrahexylammonium perchlorate ($THxAClO_4$) was prepared by metathesis of THxACl and $HClO_4$ and recrystallized twice from a mixture of ethyl acetate and ethanol.[25] Bis(triphenylphosphoranylidine)ammonium tetrakis(pentafluorophenyl)borate (BATB) was synthesized from BACl and LiTB by metathesis and recrystallized from ethanol−acetone mixture.[26] All aqueous solutions were prepared with demineralized and filtered water from ELIX system (Millipore). Argon gas was from Multax.

Apparatus and Procedures. Cyclic voltammetry (CV) and square-wave voltammetry (SWV) were performed with a Biologic Bipotentiostat SP-300. Parameters for SWV were: frequency 8 Hz, step potential 1 mV, amplitude 50 mV. All measurements were performed at room temperature (23 ± 2 °C).

For measurements with droplet-modified electrodes, a glassy carbon (GC) disc with an active area of 0.031 cm^2 was used as a working electrode. It was polished with 1, 0.3, and 0.05 μm Al_2O_3 (Buehler) slurry and sonicated in demineralized water before use. Next, a 2 μL droplet of the organic phase was deposited on the GC surface with a micropipet. So-obtained droplet-modified electrode was then immersed in the aqueous electrolyte solution. A silver−silver chloride electrode (Ag|AgCl|3 M KCl) and a Pt wire were used as reference and counter electrodes, respectively

SECM measurements were carried out with a CHI900B SECM workstation (CH Instruments). Pt microelectrodes for SECM experiments were made by sealing a Pt wire (25 μm diameter, Goodfellow, England) using PC-10 micropipet puller (Narishige) into borosilicate glass capillaries and polished. A Pt wire and Ag|AgCl|3 M KCl were counter and reference electrodes respectively, and were immersed in the aqueous phase. The measured open-circuit potential was then recalculated versus the reversible hydrogen electrode (RHE) whose potential is −0.276 V vs Ag|AgCl|3 M KCl under these conditions.[24] For the voltammetric detection of H_2O_2, a Hg|Hg_2SO_4|$K_2SO_{4(sat)}$ reference electrode was used instead of the Ag|AgCl|3 M KCl to avoid possible contribution of Cl^- oxidation to the measured current. A Pt microelectrode in the aqueous phase served as the SECM tip, and its position was controlled by stepper motors in the *X*, *Y*, and *Z* directions. To ensure anaerobic conditions, argon was bubbled through the

dx.doi.org/10.1021/jp507310d | J. Phys. Chem. C 2014, 118, 23154−23161

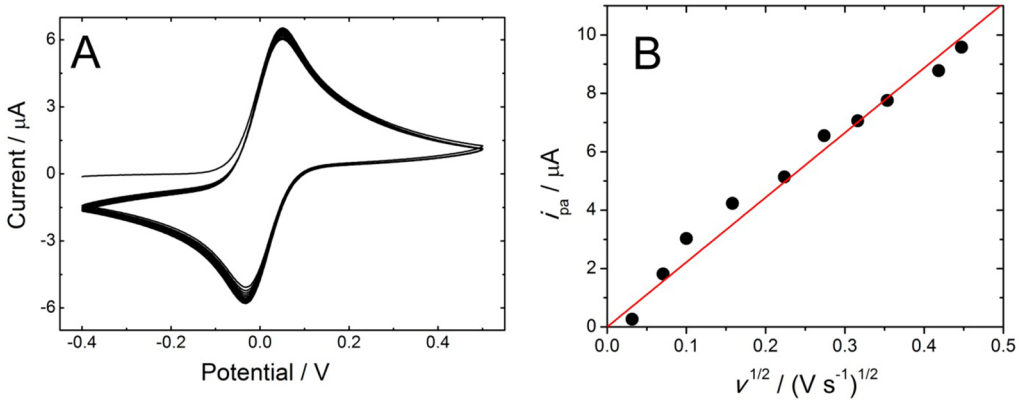

Figure 1. (A) Cyclic voltammograms (10 subsequent cycles) recorded at GC electrode coated with 2 μL of TFT solution of 1 mM DMFc and 0.1 M $THxAClO_4$. The electrode was immersed in the aqueous solution of 0.1 M $NaClO_4$. Scan rate: 50 mV s^{-1}. (B) Dependence of anodic peak current, I_{pa}, on the square root of the scan rate. The red line is a regression line (R^2 = 0.9939) with an intercept fixed at zero to follow reversibility criterion.[27]

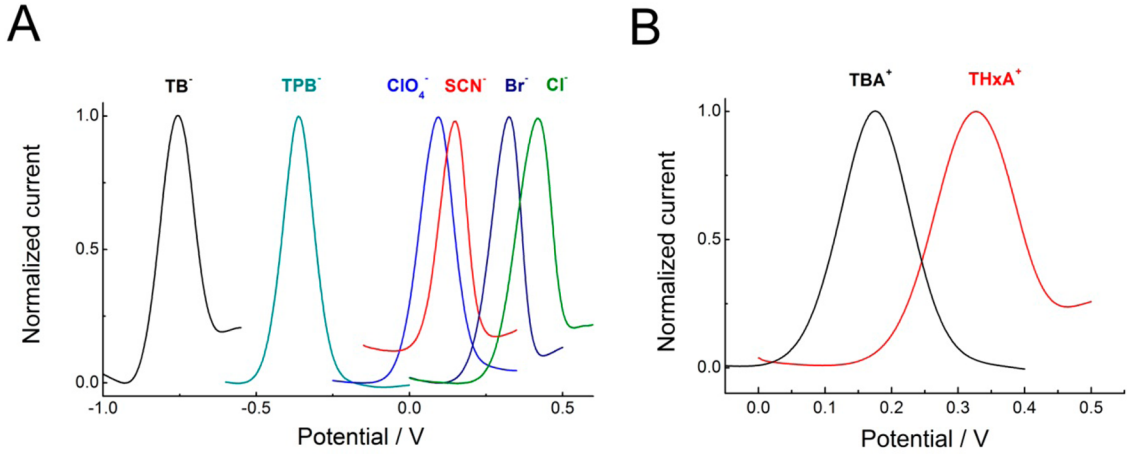

Figure 2. SWV curves recorded on thin film electrodes in the presence of different transferring anions (A) and cations (B). For compositions of the aqueous and the organic phase see Table 1

two liquid phases for 15 min before measurements, and during the measurement it was passed above the solution.

RESULTS AND DISCUSSION

Determination of $DMFc^+$/DMFc Redox Potential in TFT and Estimation of Gibbs Transfer Energies of H^+, TB^-, and ClO_4^- Ions. First, the redox potentials of $DMFc^+$/DMFc couple in TFT ($E^{\ominus}_{DMFc/DMFc^+}$) and Gibbs transfer energies of H^+, TB^-, and ClO_4^- ($\Delta^{TFT}_W G^{\ominus}_{H^+}$,$\Delta^{TFT}_W G^{\ominus}_{TB^-}$, $\Delta^{TFT}_W G^{\ominus}_{ClO_4^-}$, respectively) were determined. These parameters have not been reported previously and are crucial for interpretation of the results described in the next sections. Determination of $E^{\ominus}_{DMFc/DMFc^+}$ and Gibbs transfer energies has been performed according to methodology described by Quentel et al.[23] Briefly, square wave voltammograms (SWV) were recorded at the glassy carbon electrode coated with a droplet of TFT solution of DMFc and organic electrolyte. This electrode was immersed into the aqueous electrolyte solution. Both organic and aqueous electrolyte contained a common ion whose transfer energy was determined (Table 1).

Oxidation of DMFc in TFT droplet can be coupled to transfer of anions (An^-) or cations (Cat^+) across TFT|W interface:

$$DMFc_{(TFT)} + An^-_{(W)} \rightleftarrows DMFc^+_{(TFT)} + An^-_{(TFT)} + e^- \quad (2a)$$

$$DMFc_{(TFT)} + Cat^+_{(TFT)} \rightleftarrows DMFc^+_{(TFT)} + Cat^+_{(W)} + e^- \quad (2b)$$

If the electrochemical process is reversible, one can calculate the standard transfer potential of an ion i, $\Delta^{TFT}_W \phi^{\ominus}_i$:[19]

$$\Delta^{TFT}_W \varphi^{\ominus}_i = E_p - E^{\ominus}_{DMFc/DMFc^+} + \frac{RT}{z_i F} \ln \frac{c_i(TFT)}{c_i(W)} \quad (3)$$

where E_p is the SWV peak potential, z_i is the charge number of the transferring ion, c_i(TFT), c_i(W) are bulk concentrations of the transferring ion in TFT and W phase, respectively. Once $\Delta^{TFT}_W \phi^{\ominus}_i$ is known, one can calculate $\Delta^{TFT}_W G^{\ominus}_i$:

$$\Delta^{TFT}_W G^{\ominus}_i = -z_i F \Delta^{TFT}_W \varphi^{\ominus}_i \quad (4)$$

The value of $E^{\ominus}_{DMFc/DMFc^+}$ can be determined with extrathermodynamic assumption that $\Delta^{TFT}_W G^{\ominus}_{TPAs^+} = \Delta^{TFT}_W G^{\ominus}_{TPB^-}$, which implies that. Then one can rewrite eq 3 to obtain

dx.doi.org/10.1021/jp507310d | J. Phys. Chem. C 2014, 118, 23154−23161

$$E^{\ominus}_{DMFc/DMFc^+} = \frac{1}{2}\left[E_p(TPAs^+) + E_p(TPB^-) + \frac{RT}{F} \ln \frac{c_{TPAs+}(TFT)c_{TPB-}(W)}{C_{TPAs+}(W)c_{TPB-}(TFT)}\right] \quad (5)$$

where $E_p(TPAs^+)$ and $E_p(TPB^-)$ are peak potentials recorded when $TPAs^+$ or TPB^- are the transferred ions.

The voltammograms recorded at the electrode modified with droplet of DMFc solution in TFT, immersed in aqueous electrolyte are shown in Figure 1A. After 10 cycles the peak current is decreased by only 8% and the peak separation is constant and equal 65 mV. The peak current is proportional to the square root of the scan rate (Figure 1B), which is indicative of a diffusion-controlled process. These features indicate that the electrochemical processes of DMFc within the TFT droplets are reversible under the present experimental conditions and allow to apply eq 3 for calculation of $\Delta^{TFT}_W\phi^{\ominus}_i$.

Position of the SWV curves on the potential scale depends on the transferring anions and cations (Figure 2). The peak potential increases in the order TB^- < TPB^-< ClO_4^-< SCN^- < Br^- < Cl^- (Figure 2A). This result clearly reflects the difference in ion transfer energies; i.e., the process is facilitated in the presence of more hydrophobic anions like TB^-. In case of cation transfer from TFT to W, the peak potential is lower for more hydrophilic TBA^+ than for more hydrophobic $THxA^+$ (Figure 2B). This result indicates that the electrochemical process is facilitated by more hydrophilic cations in the organic phase.

$E^{\ominus}_{DMFc/DMFc^+}$ was calculated from eq 5 to be −0.079 V vs Ag|AgCl|3 M KCl electrode which corresponds to 0.118 V versus standard hydrogen electrode (SHE). The values of $\Delta^{TFT}_W\phi^{\ominus}_i$ and $\Delta^{TFT}_W G^{\ominus}_i$ were determined from eqs 3 and 4, and are listed in Table 1 (columns 5 and 6). To determine $\Delta^{TFT}_W G^{\ominus}_{H^+}$,

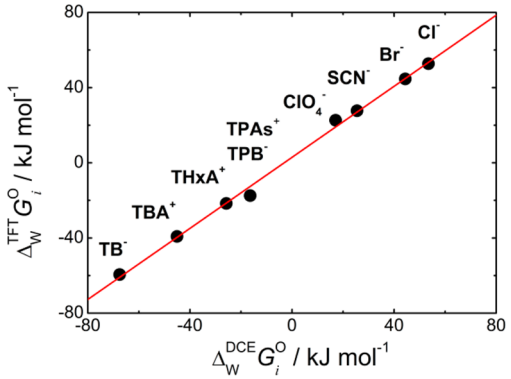

Figure 3. Dependence of $\Delta^{TFT}_W G^{\ominus}_i$ vs $\Delta^{DCE}_W G^{\ominus}_i$. The values of $\Delta^{DCE}_W G^{\ominus}_i$ were taken from ref 28.

dependence of $\Delta^{TFT}_W G^{\ominus}_i$ vs $\Delta^{DCE}_W G^{\ominus}_i$ was plotted (Figure 3). This dependence is linear and the regression line is given by

$$\Delta^{TFT}_W G^{\ominus}_i \text{ (kJ mol}^{-1}) = 0.95 \times \Delta^{DCE}_W G^{\ominus}_i \text{ (kJ mol}^{-1}) + 0.02 \quad (6)$$

By taking $\Delta^{DCE}_W G^{\ominus}_{H^+}$ = 53.1 kJ mol^{-1},[10] one calculates $\Delta^{TFT}_W G^{\ominus}_{H^+}$ = 50.5 kJ mol^{-1} which via eq 4 corresponds to $\Delta^{TFT}_W\phi^{\ominus}_{H^+}\Delta^{TFT}_W\phi^{\ominus}_{H^+}$ = −0.52 V.

Hydrogen Evolution Reaction in TFT−W Biphasic System under Anaerobic Conditions. HER study was performed in TFT−W biphasic system under anaerobic conditions with W phase containing $HClO_4$ as a proton donor and TFT phase containing DMFc as an electron donor. Both phases contained electrolytes with a common TB^- anion, as in an earlier study of HER in the DCE−W biphasic system.[10]

After 30 min of the two-phase reaction, the color of TFT phase changes from yellow to green (Figure 4, flask 1). This

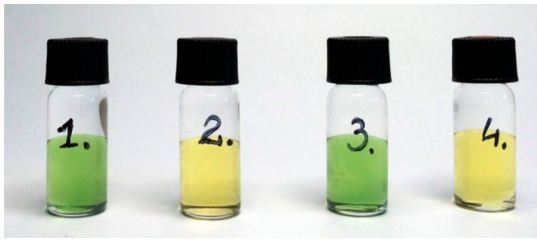

Figure 4. Photographs taken after 30 min of two-phase reaction under anaerobic conditions. **Flask 1**: 5 mM DMFc, 5 mM BATB in TFT; 5 mM LiTB, 0.1 M $HClO_4$ in W. **Flask 2**: 5 mM DMFc, 5 mM BATB in TFT; 5 mM LiTB, 0.1 M $NaClO_4$ in W. **Flask 3**: 5 mM DMFc in TFT; 5 mM LiTB, 0.1 M $HClO_4$ in W. **Flask 4**: 5 mM DMFc in TFT; 5 mM LiTB, 0.1 M $NaClO_4$ in W.

observation indicates that DMFc is oxidized to $DMFc^+$. The aqueous phase remains colorless meaning that $DMFc^+$ is not transferred from TFT to W phase during reaction. Lack of $DMFc^+$ transfer is also confirmed by stable cyclic voltammograms obtained with a droplet of DMFc solution in the TFT-modified electrode in the presence of TB^- in both phases (Figure 5). In the absence of $HClO_4$ in the aqueous phase, the

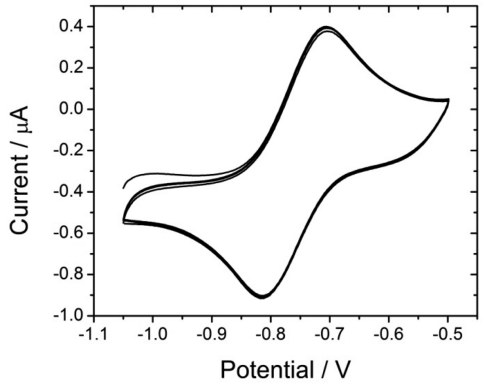

Figure 5. Cyclic voltammograms (10 cycles overlaid) recorded at GC electrode modified with 2 μL of TFT solution of 1 mM DMFC and 0.1 M BATB. The electrode was immersed in 0.01 M LiTB aqueous solution. Scan rate was 50 mV s^{-1}.

organic phase remains yellow (Figure 4, flask 2) indicating that oxidation of DMFc in TFT does not occur when there is no acid in the W phase. All these results suggest that the electron transfer reaction can be written as[5−10]

$$2DMFc_{(TFT)} + 2H^+_{(W)} \rightleftarrows 2DMFc^+_{(TFT)} + H_2 \quad (7)$$

H_2 was then detected with SECM using a Pt microelectrode tip placed in W phase above TFT|W interface, according to the described methodology.[24] Briefly, the electrode potential was measured as a function of the distance between the tip and TFT|W interface. According to the Nernst equation:

dx.doi.org/10.1021/jp507310d | J. Phys. Chem. C 2014, 118, 23154−23161

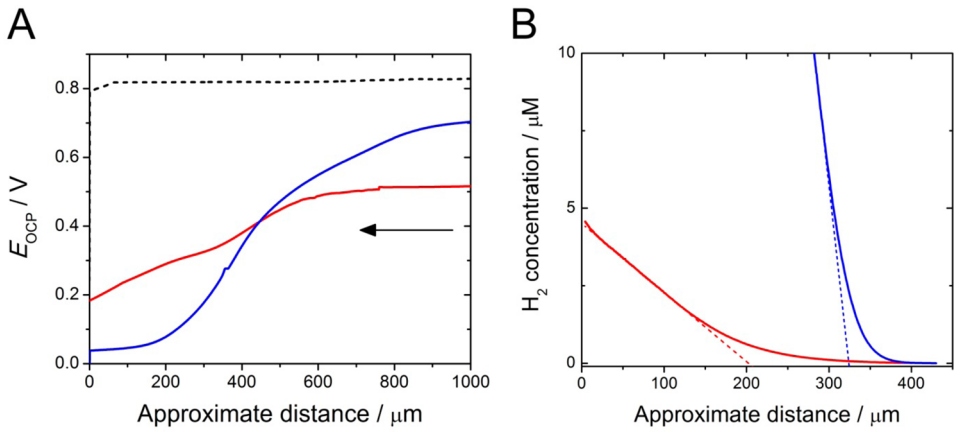

Figure 6. (A) Potentiometric approach curves to TFT−W interface recorded 30 min after interface creation under anaerobic conditions. Open-circuit potential was recalculated vs RHE (see Experimental Section). Red curve: the TFT phase contained 50 mM DMFc and 5 mM BATB while the W phase contained 0.1 M $HClO_4$ and 5 mM LiTB. Blue curve: the TFT phase contained 50 mM DMFc while the W phase contained 0.1 M $HClO_4$ and 5 mM LiTB. Dashed curve: the TFT phase contained 50 mM DMFc and 0.1 M $THxA^+ClO_4^-$ while the W phase contained 0.1 M $HClO_4$. The arrow indicates measurement direction. (B) Hydrogen concentration profiles recorded in the presence (red curve) and absence (blue curve) of BATB in TFT.

$$E = E^{\ominus}_{H_2/2H^+} + \frac{RT}{2F}\ln\frac{a_{H^+(W)}{}^2}{a_{H_2}} \quad (8)$$

the potential decreases with an increase of the H_2 activity in the W phase. As a result, a decrease of the measured potential as the tip approaches the interface liquidlliquid interface is expected.

Figure 6A shows potentiometric approach curves recorded after 30 min of the two-phase reactions. After this time, quasi-steady state conditions (H_2 diffusion profile, Figure 6B) are maintained. It should be noted that the real position of the interface could not be determined accurately from the approach curves, because the interface was bent when the tip was traveling across the interface to the organic phase.

In the studied system, the measured potential indeed decreases as the tip approaches the interface (curve red). This result confirms that H_2 is present in the aqueous phase in the vicinity of TFT|W interface. The lack of bubbles at the interface suggests that the rate of H_2 formation is lower than the rate of H_2 dissolution in water.

Whether reaction 7 is heterogeneous or homogeneous can be deduced from the comparison of the redox potentials of $DMFc/DMFc^+$ and $H_2/2H^+$ couples. Taking into account that $[E^{\ominus}_{DMFc/DMFc^+}]^{TFT}_{SHE}$ = 0.118 V (see previous section), one may conclude that DMFc dissolved in TFT is not a sufficiently strong electron donor to reduce heterogeneously H^+ dissolved in W. On the other hand, the standard redox potential of $H_2/2H^+$ in TFT vs SHE is equal:[29]

$$[E^{\ominus}_{H_2/2H^+}]^{TFT}_{SHE} = [E^{\ominus}_{H_2/2H^+}]^{W}_{SHE} - \Delta^{TFT}_{W}\varphi^{\ominus}_{H^+} = 0.52\ V \quad (9)$$

Clearly, $[E^{\ominus}_{DMFc/DMFc^+}]^{TFT}_{SHE} < [E^{\ominus}_{H_2/2H^+}]^{TFT}_{SHE}$, indicating that DMFc can reduce H^+ homogeneously in TFT:

$$2DMFc_{(TFT)} + 2H^+_{(TFT)} \rightleftarrows 2DMFc^+_{(TFT)} + H_2 \quad (10)$$

Since H^+ are initially present in W phase, proton transfer from W to TFT must precede the electron transfer step. The Galvani potential difference, $\Delta^{TFT}_{W}\phi$, (−0.447 V) (see Supporting Information) is higher than $\Delta^{TFT}_{W}\phi^{\ominus}_{H^+}$ = −0.52 V. Under such conditions, H^+ cannot be transferred from W to TFT via a simple ion transfer mechanism. However, one should consider its transfer by partitioning of neutral HTB molecule, not affected by Galvani potential difference (eq 11).

To determine whether TB^- can extract H^+ from W to TFT, we performed the two-phase reaction in the system where TB^- were initially present only in W phase. As can be seen in Figure 4 (flask 3), the organic phase changes its color from yellow to green indicating oxidation of DMFc. Under the same conditions, SECM tip potential decreases when the tip approaches TFT|W interface (Figure 6A, blue curve), indicating H_2 formation. To further prove that TB^- are essential for H^+ transfer, we performed the reaction under conditions unfavorable for homogeneous electron transfer in the absence of TB^- both in TFT and W phase. We used ClO_4^- as a potential determining ion to polarize TFT|W interface to the potential substantially higher than $\Delta^{TFT}_{W}\phi^{\ominus}_{H^+}$. According to eq 1, when electrolyte solutions in TFT and W are equimolar (0.1 M $THxA^+ClO_4^-$ in TFT and 0.1 M $HClO_4$ in W) the Galvani potential difference is $\Delta^{TFT}_{W}\phi = \Delta^{TFT}_{W}\phi^{\ominus}_{ClO_4^-}$ = 0.235 V. The lack of color change for this system (not shown) and the lack of gradual decrease of the tip potential on the SECM approach curve (Figure 6A, dashed curve), indicates that H_2 is not formed when there is no TB^- in the system. All these results show that conditions favorable for homogeneous electron transfer between electron donor and protons in TFT phase are indispensable for H_2 generation in the TFT−W biphasic system.

Globally, the process of H^+ transfer by TB^- from W to TFT can be written as

$$H^+_{(W)} + TB^-_{(W)} \rightleftarrows HTB_{(TFT)} \quad (11)$$

The mechanism of proton transfer is likely to be association of H^+ and TB^- followed by transfer of neutral HTB molecule from W to TFT. It is known as association coupled ion transfer (ACT) and has been previously reported for transfer of K^+ from W to nitrobenzene[30] and from W to DCE.[31] To determine whether reaction 11 occurs spontaneously, one has to calculate its Gibbs energy. Reaction 11 can then be split into following individual reactions:

$$H^+_{(W)} \rightleftarrows H^+_{(TFT)} \Delta^{TFT}_{W}G^{\ominus}_{H^+} \quad (12a)$$

dx.doi.org/10.1021/jp507310d | J. Phys. Chem. C 2014, 118, 23154−23161

$$TB^-_{(W)} \rightleftarrows TB^-_{(TFT)} \Delta_W^{TFT} G^{\ominus}_{TB^-} \quad (12b)$$

$$H^+_{(TFT)} + \rightleftarrows TB^-_{(TFT)} \rightleftarrows HTB_{(TFT)} \Delta_{as} G^{\ominus} \quad (12c)$$

Gibbs energy of reaction 11 is given by

$$\Delta G = \Delta_W^{TFT} G^{\ominus}_{H^+} + \Delta_W^{TFT} G^{\ominus}_{TB^-} + \Delta_{as} G^{\ominus} \quad (13)$$

Gibbs energy of association between H^+ and TB^- in TFT (reaction 12c) can be calculated from

$$\Delta_{as} G^{\ominus} = -RT \ln K_{as} \quad (14)$$

where K_{as} is the association constant given by the Fuoss equation:[32]

$$K_{as} = \frac{4000\pi N_A a^3}{3} \exp\left(\frac{e^2}{4\pi a \varepsilon_0 \varepsilon k_B T}\right) \quad (15)$$

where $a = r_{H^+} + r_{TB^-} \approx r_{TB^-}$, N_A is the Avogadro's constant, r_{H^+} and r_{H^-} are ionic radii of H^+ and TB^-, e is the elementary charge, ε_0 is the vacuum permittivity, ε is the relative permittivity of TFT, k_B is the Boltzmann constant, and T is the temperature. By taking $r_{TB^-} \approx r_{TPB^-} = 0.421$ nm[33] and $\varepsilon = 9.2$,[18] one calculates $\Delta_{as} G^{\ominus} = -31.8$ kJ mol^{-1}. Then, by taking $\Delta_W^{TFT} G^{\ominus}_{H^+} = 50.5$ kJ mol^{-1} and $\Delta_W^{TFT} G^{\ominus}_{TB^-} = -59.4$ kJ mol^{-1} estimated in the previous section, one obtains (eq 13) $\Delta G = -40.7$ kJ mol^{-1}. Negative value indicates that ACT process described by reaction 11 is indeed spontaneous. We have determined (see Supporting Information) that TB^- anions extract protons to TFT stoichiometrically and the degree of HTB dissociation in TFT is 2%. Such low dissociation degree still provides detectable concentration of H_2 in water (Figure 6B), because the ongoing reaction 10 shifts HTB dissociation equilibrium toward formation of H^+ in TFT.

To determine whether HTB dissociation equilibrium affects HER, one can consider the influence of the presence of BATB in TFT on H_2 flux. In the presence of BATB, HTB dissociation equilibrium should be shifted toward formation of HTB, and the concentration of H^+ in TFT should be lower than in the absence of BATB. Low H^+ concentration in TFT should decrease the homogeneous electron transfer rate and the resulting H_2 flux should be lower.

To calculate H_2 flux, potentiometric approach curves (curves red and blue in Figure 6A) were replotted in H_2 concentration vs distance coordinates (Figure 6B). H_2 concentration at a given distance (c_{H_2}) was calculated from the measured open circuit potential (E_{OCP}) from[24]

$$c_{H_2} = \frac{\exp\left(-\frac{2FE_{OCP}}{RT}\right)}{k_H} \quad (16)$$

where k_H is the Henry's constant (1282 dm^3 atm mol^{-1}).[34] The dependences shown in Figure 6B are approximately linear at short distances with the slopes of $((\delta c_{H_2})/(\delta_x)) = -2.2 \times 10^{-7}$ mol cm^{-4} (curve red) and $((\delta c_{H_2})/(\delta_x)) = -2.3 \times 10^{-6}$ mol cm^{-4} (curve blue) in the presence and absence of BATB, respectively. Once the concentration gradients, $((\delta c_{H_2})/(\delta_x))$, are known, the H_2 flux, J_{H_2}, can be calculated from the Fick's first law

$$J_{H_2} = -D_{H_2}\left(\frac{\delta c_{H_2}}{\delta x}\right) \quad (17)$$

where D_{H_2} is the diffusion coefficient of H_2 (4.5×10^{-5} cm^2 s^{-1}).[35] The calculated J_{H_2} is 1 order of magnitude smaller in the presence of BATB (10^{-11} vs 10^{-10} mol cm^{-2} s^{-1}). This result confirms that HER rate is affected by the dissociation of the weak acid HTB in TFT. Since the H_2 flux is higher when the dissociation equilibrium is shifted toward formation of H^+ in TFT, one can conclude that the homogeneous electron transfer occurs between DMFc and H^+, and not between DMFc and HTB. In the latter case, J_{H_2} would be higher in the presence of BATB. The hydrogen flux in the absence of BATB is of the same order of magnitude as for the earlier studied DCE–W biphasic system,[24] indicating clearly that unsupported TFT can replace DCE for HER at ITIES. This result proves that the biphasic system can be simplified by elimination of BATB electrolyte from the organic phase.

Hydrogen Peroxide Generation at TFT|W Interface under Aerobic Conditions. Formation of H_2O_2 under aerobic conditions is described by the reaction[11−13]

$$2DMFc + O_2 + 2H^+ \rightleftarrows 2DMFc^+ + H_2O_2 \quad (18)$$

It has been found earlier that in the presence of O_2 and H^+ in the organic phase, H_2O_2 is formed via homogeneous electron transfer (HomET) in the bulk organic phase and at the same time via heterogeneous ET (HetET) at the liquid|liquid interface.[11−13] To determine whether HomET or HetET dominates, we performed two-phase reactions in the presence and in the absence of LiTB in W. In the presence of LiTB, the ACT mechanism of H^+ transfer ensures conditions for both HetET and HomET, whereas in the absence of LiTB, reaction 18 proceeds only as HetET at the TFT|W interface. By comparing the amount of H_2O_2 formed under both conditions, one can conclude whether HetET or HomET is a dominant reaction path.

Both in the presence and in the absence of LiTB in W, the organic phase turned green after 24 h (Figure 7, row 1 flask 7 and 9) and the aqueous phase turned purple after addition of

Figure 7. Photographs of shake-flask experiments after 24 h of the two-phase reaction. In row 1 the bottom phase is 5 mM DMFc in TFT solution. The upper phase in row 1 is flask 7:0.1 M $HClO_4$ aq; flask 8:0.1 M $NaClO_4$ aq, flask 9:5 mM LiTB, 0.1 M $HClO_4$. In row 2 are the aqueous phases (0.5 mL) taken from systems presented in row 1 after addition of 200 μL of 0.1 M KI and 10% starch.

dx.doi.org/10.1021/jp507310d | J. Phys. Chem. C 2014, 118, 23154−23161

KI and starch (Figure 6, row 2, flask 7 and 9), indicating formation of H_2O_2 in the reaction:

$$3I^- + H_2O_2 + 2H^+ \rightarrow I_3^- + H_2O \quad (19)$$

In the absence of $HClO_4$ in the aqueous phase, the organic phase remained yellow after 24 h (Figure 7, row 1 flask 8) and no color change was observed after addition of KI and starch to the aqueous phase (Figure 7, row 2, flask 8). This observation indicates that in the absence of acid in W phase, H_2O_2 is not formed and DMFc is not oxidized by molecular oxygen.

gNext, the electrochemical detection of H_2O_2 in both systems was attempted with a Pt microelectrode located ca. 1 mm above the interface (Figure 8A). The anodic current at 0.7

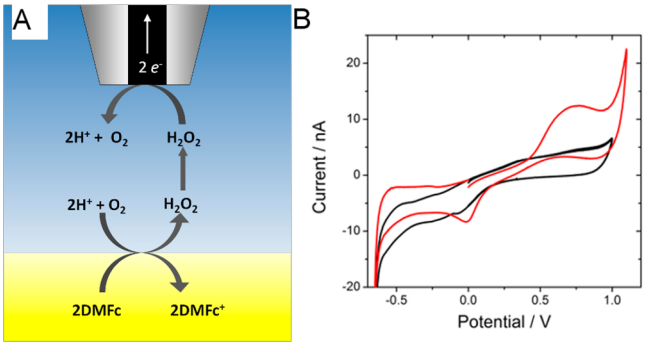

Figure 8. (A) Schematic representation of H_2O_2 electrochemical detection close to the TFT|W interface. (B) Cyclic voltammograms recorded ca. 1 mm above TFT|W interface. The TFT phase contained 5 mM DMFc, while the W phase contained 0.1 M $HClO_4$ (curve black) or 0.1 M $HClO_4$ + 5 mM LiTB (curve red).

V due to H_2O_2 oxidation is an order of magnitude higher in the presence of LiTB (Figure 8B, red curve) than in the absence of LiTB (Figure 8B, black curve). This result indicates that the amount of H_2O_2 formed in HomET is larger than in HetET. The reason is probably because HomET occurs in a certain volume of organic phase, whereas HetET occurs only at ITIES plane. In the former case, a higher number of molecules can interact. Another reason can be the higher standard potential of O_2/H_2O_2 couple in TFT than in W. Although its value is unknown in TFT, it is indeed higher in a similar solvent, DCE ($E^{\ominus}_{O_2/H_2O_2}$ = 1.165 V) than in water ($E^{\ominus}_{O_2/H_2O_2}$ = 0.695 V).[29] Higher $E^{\ominus}_{O_2/H_2O_2}$ in the organic solvent reflects the fact that the oxygen reduction eliminates protons from the solution, and the reaction is thermodynamically more favorable in the organic solvent where the ion solvation energies are generally lower than in water.[33] As a result, the driving force for HomET is higher than for HetET which then explains why the HomET path dominates in the studied system.

CONCLUSIONS

The results obtained in this work clearly shows that 1,2-dichloroethane can be replaced by a less toxic trifluorotoluene (TFT) for generation of H_2 or H_2O_2 in a liquid−liquid biphasic system.

The mechanism of both reactions, especially the role of electrolyte present in aqueous phase was elucidated. During H_2 generation, electron transfer between electron donor and protons occurs in the TFT phase adjacent to the interface. When hydrophobic TB^- anions are present in water, protons are transferred to TFT in the form of HTB acid via ion pair transfer. For this reason, H^+ transfer is independent of the Galvani potential difference between two liquid phases. Importantly, H_2 generation is facilitated by HTB dissociation in TFT and is faster in the absence of hydrophobic BATB salt in TFT. This result simplifies the biphasic system by elimination of potential determining ions, providing that the aqueous phase contains a phase transfer catalyst.

The same mechanism operates during H_2O_2 generation under aerobic conditions. When TB^- are present in the aqueous phase, a homogeneous electron transfer in TFT dominates over the heterogeneous electron transfer across TFT|W interface.

To discuss the thermodynamics of H_2 and H_2O_2 generation, Gibbs energies of transfer for a wide variety of inorganic anions across the TFT|W interface have been determined and their order is similar to other organic-water systems studied earlier.[23,36,37]

ASSOCIATED CONTENT

Supporting Information

Calculations of the Galvani potential difference and concentrations of H^+ and HTB in TFT. This material is available free of charge via the Internet at http://pubs.acs.org.

AUTHOR INFORMATION

Corresponding Authors

*(W.A.) E-mail: wadamiak@ichf.edu.pl.
*(M.O.) E-mail: mopallo@ichf.edu.pl.

Notes

The authors declare no competing financial interest.

ACKNOWLEDGMENTS

We thank Dr. Martin Jonsson-Niedziołka from the Institute of Physical Chemistry, PAS, for his valuable comments about the manuscript. Project "PSPB-035/2010: Electrocatalysis at Droplets" was supported by a grant from Switzerland through the Swiss Contribution to the enlarged European Union.

REFERENCES

(1) Stolten, D. *Hydrogen and Fuel Cells: Fundamentals, Technologies and Applications*; John Wiley & Sons: Weinheim, Germany, 2010.
(2) Jones, C. W. *Applications of Hydrogen Peroxide and Derivatives*; Royal Society of Chemistry: Cambridge, U.K., 1999.
(3) Holladay, J. D.; Hu, J.; King, D. L.; Wang, Y. An Overview of Hydrogen Production Technologies. *Catal. Today* **2009**, *139*, 244−260.
(4) Campos-Martin, J. M.; Blanco-Brieva, G.; Fierro, J. L. G. Hydrogen Peroxide Synthesis: An Outlook Beyond the Anthraquinone Process. *Angew. Chem., Int. Ed.* **2006**, *45*, 6962−6984.
(5) Ge, P.; Olaya, A. J.; Scanlon, M. D.; Patir, I. H.; Vrubel, H.; Girault, H. H. Photoinduced Biphasic Hydrogen Evolution: Decamethylosmocene as a Light-Driven Electron Donor. *ChemPhysChem* **2013**, *14*, 2308−2316.
(6) Bian, X.; Scanlon, M. D.; Wang, S.; Liao, L.; Tang, Y.; Liu, B.; Girault, H. H. Floating Conductive Catalytic Nano-Rafts at Soft Interfaces for Hydrogen Evolution. *Chem. Sci.* **2013**, *4*, 3432−3441.
(7) Ge, P.; Scanlon, M. D.; Peljo, P.; Bian, X.; Vrubel, H.; O'Neill, A.; Coleman, J. N.; Cantoni, M.; Hu, X.; Kontturi, K.; et al. Hydrogen Evolution across Nano-Schottky Junctions at Carbon Supported MoS_2 Catalysts in Biphasic Liquid Systems. *Chem. Commun.* **2012**, *48*, 6484−6486.
(8) Hatay, I.; Ge, P. Y.; Vrubel, H.; Hu, X.; Girault, H. H. Hydrogen Evolution at Polarised Liquid/Liquid Interfaces Catalyzed by Molybdenum Disulfide. *Energy Environ. Sci.* **2011**, *4*, 4246−4251.

(9) Nieminen, J. J.; Hatay, I.; Ge, P. Y.; Mendez, M. A.; Murtomaki, L.; Girault, H. H. Hydrogen Evolution Catalyzed by Electrodeposited Nanoparticles at the Liquid/Liquid Interface. *Chem. Commun.* **2011**, *47*, 5548−5550.
(10) Hatay, I.; Su, B.; Li, F.; Partovi-Nia, R.; Vrubel, H.; Hu, X.; Ersoz, M.; Girault, H. H. Hydrogen Evolution at Liquid-Liquid Interfaces. *Angew. Chem., Int. Ed.* **2009**, *48*, 5139−5142.
(11) Jedraszko, J.; Nogala, W.; Adamiak, W.; Rozniecka, E.; Lubarska-Radziejewska, I.; Girault, H. H.; Opallo, M. Hydrogen Peroxide Generation at Liquid|Liquid Interface under Conditions Unfavorable for Proton Transfer from Aqueous to Organic Phase. *J. Phys. Chem. C* **2013**, *117*, 20681−20688.
(12) Li, F.; Su, B.; Salazar, F. C.; Partovi Nia, R.; Girault, H. H. Detection of Hydrogen Peroxide Produced at a Liquid/Liquid Interface Using Scanning Electrochemical Microscopy. *Electrochem. Commun.* **2009**, *11*, 473−476.
(13) Su, B.; Partovi Nia, R.; Li, F.; Hojeij, M.; Prudent, M.; Corminboeuf, C.; Samec, Z.; Girault, H. H. H_2O_2 Generation by Decamethylferrocene at a Liquid/Liquid Interface. *Angew. Chem., Int. Ed.* **2008**, *47*, 4675−4678.
(14) Volkov, A. G.; Deamer, D. W. *Liquid-Liquid Interfaces: Theory and Methods*; CRC Press: Boca Raton, FL, 1996.
(15) Su, B.; Hatay, I.; Ge, P. Y.; Mendez, M.; Corminboeuf, C.; Samec, Z.; Ersoz, M.; Girault, H. H. Oxygen and Proton Reduction by Decamethylferrocene in Non-Aqueous Acidic Media. *Chem. Commun.* **2010**, *46*, 2918−2919.
(16) Scanlon, M. D.; Bian, X.; Vrubel, H.; Amstutz, V.; Schenk, K.; Liu, B.; Girault, H. H. Low-Cost Industrially Available Molybdenum Boride and Carbide as "Platinum Like" Catalysts for Hydrogen Evolution Reaction in Biphasic Liquid Systems. *Phys. Chem. Chem. Phys.* **2013**, *15*, 2847−2857.
(17) *IARC Monographs on the Evaluation of Carcinogenic Risks to Humans*; IARC Press: Lyon, France, 1999; Vol. *71*, part 2.
(18) Olaya, A. J.; Ge, P.; Girault, H. H. Ion Transfer Across Trifuorotoluene|Water Interface. *Electrochem. Commun.* **2012**, *19*, 101−104.
(19) Ogawa, A.; Curran, D. P. Benzotrifluoride: A Useful Alternative Solvent for Organic Reactions Currently Conducted in Dichloromethane and Related Solvents. *J. Org. Chem.* **1997**, *62*, 450−451.
(20) Kadish, K. M.; Anderson, J. E. Purification of Solvents for Electroanalysis: Benzonitrile, Dichloromethane, 1,1-Dichloroethane, and 1,2-Dichloroethane. *Pure Appl. Chem.* **1987**, *59*, 703−714.
(21) Knochel, P. *Modern Solvents in Organic Synthesis*; Springer-Verlag: Berlin and Heidelberg, Germany, 1999.
(22) Thomas, J. C.; Trend, J. E.; Rakow, N. A.; Wendland, M. S.; Poirier, R. J.; Paolucci, D. M. Optical Sensor for Diverse Organic Vapors at ppm Concentration Ranges. *Sensors* **2011**, *11*, 3267−3280.
(23) Quentel, F.; Mirceski, V.; Elleouet, C.; L'Her, M. Studying the Thermodynamics and Kinetics of Ion Transfers Across Water-2-Nitrophenyloctyl Ether Interface by Means of Organic-Solution-Modified Electrodes. *J. Phys. Chem. C* **2008**, *112*, 15553−15561.
(24) Jedraszko, J.; Nogala, W.; Adamiak, W.; Girault, H. H.; Opallo, M. Scanning Electrochemical Microscopy Determination of Hydrogen Flux At Liquid|Liquid Interface with Potentiometric Probe. *Electrochem. Commun.* **2014**, *43*, 22−24.
(25) House, H.; Feng, E.; Peet, N. Comparison of Various Tetraalkylammonium Salts as Supporting Electrolytes in Organic Electrochemical Reactions. *J. Org. Chem.* **1971**, *36*, 2371−2375.
(26) Olaya, A. J.; Mendez, M. A.; Cortes-Salazar, F.; Girault, H. H. Voltammetric Determination of Extreme Standard Gibbs Ion Transfer Energy. *J. Electroanal. Chem.* **2010**, *644*, 60−66.
(27) Bard, A. J.; Faulkner, L. R. *Electrochemical Methods: Fundamentals and Applications*; John Wiley & Sons: New York, 2001.
(28) Czapkiewicz, J.; Czapkiewicz-Tutaj, B. Relative Scale of Free Energy of Transfer of Anions from Water to 1,2-Dichloroethane. *J. Chem. Soc. Faraday Trans. 1* **1980**, *76*, 663.
(29) Nia, R. P. *Electrocatalysis at Liquid-Liquid Interfaces*; Ph.D. Thesis. Ecole Polytechnique de Lausanne: Lausanne, Switzerland, 2010.
(30) Yoshida, Z.; Freiser, H. Mechanism of the Carrier-Mediated Transport of Potassium Ion Across Water-Nitrobenzene Interface by Valinomycin. *J. Electroanal. Chem.* **1984**, *179*, 31−39.
(31) Sinru, L.; Zaofan, Z.; Freiser, H. Potassium Ion Transport Processes Across the Interface of an Immiscible Liquid Pair in the Presence of Crown Ethers. *J. Electroanal. Chem.* **1986**, *210*, 137−146.
(32) Fuoss, R. M. Ionic Association. III. The Equilibrium Between Ion Pairs and Free Ions. *J. Am. Chem. Soc.* **1958**, *80*, 5059−5061.
(33) Volkov, A. E. G. *Liquid Interfaces in Chemical, Biological and Pharmaceutical Applications*; Marcel Dekker: New York, 2001.
(34) Khan, S. A.; Duraiswamy, S. Controlling Bubbles Using Bubbles-Microfluidic Synthesis of Ultra-Small Gold Nanocrystals with Gas-Evolving Reducing Agents. *Lab Chip* **2012**, *12*, 1807−1812.
(35) Mazarei, A. F.; Sandall, O. C. Diffusion Coefficients for Helium, Hydrogen, and Carbon Dioxide in Water at 25°C. *AlChE J.* **1980**, *26*, 154−157.
(36) Shul, G.; Opallo, M.; Marken, F. Liquid-Liquid Interfacial Processes at Hydrophobic Silica Carbon Composite Electrodes: Ion Transfer at Water-Nitrobenzene, Water-o-Nitrophenyloctylether, and at Water-o-Nitrophenylphenylether Interfaces. *Electrochim. Acta* **2005**, *50*, 2315−2322.
(37) Komorsky-Lovric, S.; Lovric, M.; Scholz, F. Cyclic Voltammetry of Decamethylferrocene at the Organic Liquid|Aqueous Solution| Graphite Three-Phase Junction. *J. Electroanal. Chem.* **2001**, *508*, 129−137.